Anal. Chem. **2002,** *74,* 4558−4565

A Microscale-Molecular Weight Sensor: Probing Molecular Diffusion between Adjacent Laminar Flows by Refractive Index Gradient Detection

Colin D. Costin and Robert E. Synovec*

Center for Process Analytical Chemistry (CPAC), Department of Chemistry, Box 351700, University of Washington, Seattle, Washington 98195-1700

A detection scheme that measures the refractive index gradient (RIG) between adjacent laminar flows in a microfluidic device has been used to develop a microscale-molecular weight sensor. The behavior of low Reynolds number flows has been well documented and shows that molecular transport (mixing) between adjacent laminar flows occurs by molecular diffusion between flow boundaries. A diode laser beam, incident upon and illuminating the entire width of a microchannel, measured the transverse concentration gradient at two different positions along a microchannel. The concentration gradient is impacted by the transverse diffusion from a flow with analyte into a flow initially without analyte. The RIG that forms as analyte diffuses from one adjacent flow to the other causes the laser beam, impinging orthogonal to the RIG through the microchannel, to be deflected. The angle of deflection is then monitored on a position-sensitive detector (PSD) at two different positions along the axis of flow to provide a measurement of analyte diffusion. The two positions are just after the flow initially without analyte merges with the flow initially containing all of the analyte (upstream) and then after the two streams have had more time to diffuse together (downstream). The ratio of the PSD signals obtained at the two positions along the flow, downstream signal divided by the upstream signal, is readily correlated to the analyte diffusion coefficient and, thus, the analyte molecular weight for a given class of compounds. The device was evaluated as a molecular weight sensor for poly(ethylene glycol) (PEG) solutions over a molar mass range from 106 to 22 800 g/mol. The ratio signal was found to be both independent of PEG concentration and sensitive to molecular weight changes for samples ranging from 960 to 22 800 g/mol. Independence of concentration is important for obtaining a reliable molecular weight measurement. The limit of detection for 11 840 g/mol PEG measured at the upstream detection position was determined to be 56 ppm, equivalent to 4.5 $\times$ 10^{-6} RI (3σ). This technique provides a much needed universal detection method, without requiring analyte derivatization chemistry (e.g., fluorescence), for microfluidic analyses that are becoming increasingly useful in monitoring chemical systems such as continuous-flow reactors or batch polymerization processes. Thus, the molecular weight determination capability is potentially applicable to other compound classes, such as DNA or proteins.

The physical properties of polymers determine the applications for which they are best suited and can also describe the quality of the synthetic products. With the increased use of specialized polymers in the world today, the need for fast and accurate analysis of their physical properties is greater than ever. One of the most critical characteristics of a polymer is its molecular weight or size, which allows polymers to have such a diverse number of applications. A number of techniques are currently used for molecular weight determinations of synthetic polymers including viscometry,[1,2] size exclusion chromatography,[3] mass spectrometry,[4] and light scattering.[1,5−7] These techniques can provide accurate molecular weight determinations; however, they can be either time-consuming, require significant sample preparation, or be limited to a high molecular weight range. Also, industrial quality control applications require faster analysis methods that can be implemented on-line, in the process environment. This niche provides an opportunity for the application of micro-total analysis systems (μ-TAS), where sampling, derivatization, separation, and detection can all be handled by a single miniaturized system. Development of μ-TAS have led to improved analysis speed and efficiency by taking advantage of the very small sample volumes characteristic of such systems. This environment quickly turns chemical information into electronic information, thus increasing the system throughput. [8]

In this work, the principles of flow injection analysis (FIA)[9] have been explored as a way to create a fast molecular weight analyzer in a microfluidic format that can be used in the process analysis environment. In microfluidic devices, the operating flow

* To whom correspondence should be addressed. E-mail: synovec@macmail.chem.washington.edu.

(1) Campbell, D.; Pethrick, R. A.; White, J. R. *Polymer Characterization Physical Techniques*, 2 ed.; Stanley Thornes Ltd: Cheltenham, U.K., 2000.
(2) Mao, Y.; Wei, W.; Zhang, J.; Yijin, L. *J. Appl. Polym. Sci.* **2001**, *82*, 63−69.
(3) Sebastian, J. M.; Register, R. A. *J. Appl. Polym. Sci.* **2001**, *82*, 2056−2069.
(4) Smith, P. B.; Pasztor, A. J.; McKelvy, M. L.; Meunier, D. M.; Froelicher, S. W.; Wang, F. C. Y. *Anal. Chem.* **1999**, *71*, 61R−80R.
(5) Suzuki, H.; Nakamura, M.; Ofusa, Y. *Chromatography* **1995**, *16*, 245−247.
(6) Alvarez, M. L.; Gras, L.; Canals, A. *Polym. Anal. Degrad.* **2000**, 253−263.
(7) Wyatt, P. J. *Anal. Chim. Acta* **1993**, *272*, 1−40.
(8) Manz, A.; Graber, N.; Widmer, H. M. *Sens. Actuators* **1990**, *B1*, 244−248.
(9) Ruzicka, J.; Hansen, E. H. *Flow Injection Analysis*; J. Wiley & Sons: New York, 1981.

10.1021/ac020143z CCC: $22.00
Published on Web 07/30/2002

conditions are readily tuned to operate in the laminar flow regime. This is due to the extremely low Reynolds numbers that generally exist for fluid streams in microchannels, where laminar flows do not exhibit turbulent mixing and the streamlines run parallel down a given channel. Thus, the mixing of two adjacent streams in a microfluidic device is dominated by diffusion of the molecular species from one stream to another.[10,11]

A microfluidic device called the T-sensor was recently developed to measure the diffusion coefficients of proteins by monitoring the diffusion of analytes between two adjacent flows in a microchannel, using laser-induced fluorescence (LIF) for detection.[12−14] Here we build upon the T-sensor work, introducing a microscale-molecular weight sensor (μ-MWS) that should provide complementary applicability. In contrast to the T-sensor development, in our system, the concentration gradient between two adjacent flows is measured directly through the refractive index gradient (RIG) and analyte chemical derivatization is not required. Thus, the μ-MWS provides universal detection that would require reasonably well characterized samples in order to provide satisfactory selectivity (e.g., process analysis applications) or some kind of separation process before detection (e.g., chromatography). Furthermore, the current configuration of the T-sensor uses a one-dimensional fit of the data, via an empirical model, to determine the analyte diffusion coefficient. Whereas, the μ-MWS reported herein has the advantage of measuring analyte diffusion at any two selected positions along the channel to determine the diffusion coefficient via a calibration curve prepared from standards of a given class of compounds and relating this calibration to molecular weight.

Refractive index (RI) detection has been widely used in traditional-scale HPLC and CE for many years,[15−25] and more recently, RI detection has been developed for microscale analysis.[26−30] This universal technique has been widely used to analyze polymers, sugar, proteins, and other analytes that do not appreciably absorb or fluoresce. A RI-based detector originally developed by Pawliszyn provided very sensitive measurements of the RIG created by the axial concentration gradient of an analyte as it passes through a capillary.[20−22] This system probed the RIG by measuring the deflection angle of a laser beam. RIG detection has also been developed where the radial concentration gradient was probed.[23−25] The data were found to be dependent on the diffusion coefficient of the analyte, and thus the molecular weight, when the appropriate FIA sample introduction conditions were met.[31,32] The scale of this previous molecular weight sensor system was significantly larger compared to the μ-MWS dimensions we report here. Furthermore, the time scale for the molecular weight determination was longer, ~90 s[31,32] versus 3 s with the μ-MWS described here.

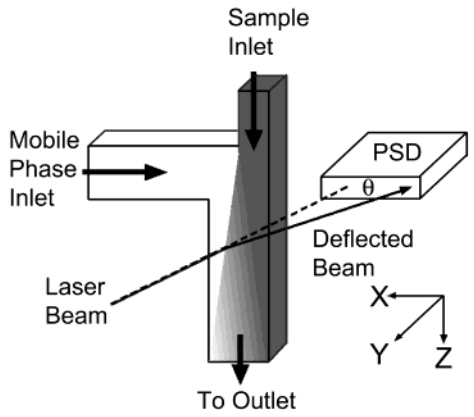

Figure 1. Illustration of the RIG measurement by the deflection of a diode laser beam on a PSD. The diode laser beam is incident upon the channel structure, orthogonal to both the direction of flow and the concentration gradient. An analyte stream (dark, for illustration purposes only) flowing in from the sampling channel meets a mobile-phase stream (light), and they flow through the analysis channel as analyte diffuses into the mobile-phase stream. A laser beam passing through the microchannel and incident on a PSD is deflected from a default position (dashed line) by the RIG between the sample and mobile-phase streams. The deflection signal θ is measured.

The μ-MWS we describe here relies upon a novel detection technique recently developed[33] that measures the RIG created in a microchannel as two adjacent streams mix by transverse diffusion (Figure 1). The deflection angle of the diode laser beam is then determined from the displacement of the beam on a position-sensitive detector (PSD). Here, the system has been further developed into a μ-MWS by making RIG measurements at two different positions along the flow axis of a microfabricated analysis channel. The first measurement is made at an upstream position just past the point where a stream with analyte merges with a stream that initially has only mobile-phase solvent. The second measurement is made at another position, downstream, closer to the end of the channel after the analyte molecules have had a significant amount of time to diffuse into the adjacent stream. A series of poly(ethylene glycol) (PEG) standards of varying molecular weight, from 106 to 22 000, served as model compounds

(10) Kovacs, G. T. A. *Micromachined Transducers Sourcebook*; WCB McGraw-Hill: Boston, 1998.
(11) Knight, J. B.; Vishwanath, A.; Brody, J. P.; Austin, R. H. *Phys. Rev. Lett.* **1998**, *80*, 3863−3866.
(12) Brody, J. P.; Kamholz, A. E.; Yager, P. *Proc. Micro. Nano-fabricated Electro-Opt. Mech. Systems Biomed. Environ. Appl.* **1997**, 103−110.
(13) Kamholz, A. E.; Weigl, B. H.; Finlayson, B. A.; Yager, P. *Anal. Chem.* **1999**, *71*, 5340−5347.
(14) Kamholz, A. E.; Yager, P. *Biophys. J.* **2001**, *80*, 155−160.
(15) Woodruff, S. D.; Yeung, E. S. *Anal. Chem.* **1982**, *54*, 1174−1178.
(16) Bornhop, D. J.; Dovichi, N. J. *Anal. Chem.* **1986**, *58*, 504−505.
(17) Bornhop, D. J.; Dovichi, N. J. *Anal. Chem.* **1987**, *59*, 1632−1636.
(18) Synovec, R. E. *Anal. Chem.* **1987**, *59*, 2877−2884.
(19) Bruno, A. E.; Krattiger, B.; Maystre, F.; Widmer, H. M. *Anal. Chem.* **1991**, *63*, 2689−2697.
(20) Pawliszyn, J. *Anal. Chem.* **1986**, *58*, 3207−3215.
(21) Pawliszyn, J.; Weber, M. F.; Dignam, M. J.; Mandelis, A.; Venter, R. D.; Park, S. *Anal. Chem.* **1986**, *58*, 236−238.
(22) Pawliszyn, J. *Anal. Chem.* **1988**, *60*, 2796−2801.
(23) Hancock, D. O.; Renn, C. N.; Synovec, R. E. *Anal. Chem.* **1990**, *62*, 2441−2447.
(24) Renn, C. N.; Synovec, R. E. *J. Chromatogr., A* **1991**, *536*, 289−301.
(25) Lima, L. R.; Synovec, R. E. *Anal. Chem.* **1993**, *65*, 128−134.
(26) Vahey, P. G.; Smith, S. A.; Costin, C. D.; Xia, Y.; Brodsky, A.; Burgess, L. W.; Synovec, R. E. *Anal. Chem.* **2002**, *74*, 177−184.
(27) Swinney, K.; Markov, D.; Bornhop, D. J. *Anal. Chem.* **2000**, *72*, 2690−2695.
(28) Puyol, M.; del Valle, M.; Garces, I.; Villuindas, F.; Dominguez, C.; Alonso, J. *Anal. Chem.* **1999**, *71*, 5037−5044.
(29) Heideman, R. G.; Veldhuis, G. J.; Jager, E. W. H.; Lambeck, P. V. *Sens. Actuators, B* **1996**, *35−36*, 234−240.
(30) Burggraf, N.; Krattiger, B.; de Mello, A. J.; de Rooij, N. F.; Manz, A. *Analyst* **1998**, *123*, 1443−1447.
(31) Murugaiah, V.; Synovec, R. E. *Anal. Chim. Acta* **1991**, *246*, 241−249.
(32) Murugaiah, V.; Synovec, R. E. *Anal. Chem.* **1992**, *64*, 2130−2137.
(33) Costin, C. D.; Synovec, R. E. *Talanta*, in press.

to study and demonstrate the capability of the system to make molecular weight determinations.

THEORY

The angular deflection of a nonabsorbed laser beam incident on a RIG is given in terms of the RIG and the concentration gradient by eq 1,[21] where θ is the angle of deflection, L is the

$$\theta = \frac{L}{n_o}\frac{dn}{dx} = \frac{L}{n_o}\frac{dn}{dC}\frac{dC}{dx} \quad (1)$$

path length of the incident beam orthogonal to the RIG, n_o is the refractive index of the solvent, and dn/dx is the change in refractive index across a flow channel, i.e., the RIG being measured. Figure 1 shows a detailed view of a small section of the microfabricated sampling system in the area where the two fluid streams merge. The laser beam is incident on the microchannel orthogonal to the flow of both streams in the *z* direction and the concentration gradient created as analyte diffuses toward the mobile-phase stream in the *x* direction. Equation 1 is rigorously defined for an incident, collimated beam that is substantially more narrow than the concentration gradient being measured. In the work reported herein, the probe beam was more than fully illuminating the channel in which the concentration gradient was located; thus, the detected RIG signal is defined by the convolution integral of the beam intensity profile over the concentration gradient. Essentially, a spatially averaged θ is measured for a given concentration gradient.

The mixing of two adjacent streams in a microfluidic device may occur by the diffusion of a molecular species from one stream to the other. The transverse diffusion between the streams generates a concentration gradient along the *x* direction (Figure 1) that is orthogonal to the flow down the analysis channel in the *z* direction. Fick's law provides a model for the time-dependent change in concentration of an analyte in one dimension that can be expressed by eq 2,[34] where C is concentration, D is the diffusion

$$\frac{dC}{dt} = \frac{d}{dx}\left(D\frac{dC}{dx}\right) \quad (2)$$

coefficient, x is the direction of net migration of the analyte, and t is the operative time scale in the μ-MWS analysis channel (Figure 2). For a given D and initial C entering the analysis channel, dC/dx will decrease as residence time on the μ-MWS increases, i.e., as sample passes through the analysis channel in the *z* direction of Figures 1 and 2. Thus, as solution containing analyte continues to migrate in the *x* direction, the concentration gradient will also change as related to the RIG defined by eq 3.[21] This shows the

$$\frac{dn}{dx} = \frac{dn}{dC}\frac{dC}{dx} \quad (3)$$

RIG is a function of both the change in RI as a function of concentration and the change in concentration as a function of position (i.e., as a function of the residence time within the analysis channel). By measuring the angle, θ, as defined by eq 1 at two positions (Figure 2) along the *z* axis (shown in Figure 1 and taking the ratio of the angles θ(downstream)/θ(upstream), an empirical relationship to analyte diffusion coefficient is obtained. For a given class of compounds, this relationship to diffusion coefficient can be directly correlated to molecular weight for a given class of compounds.

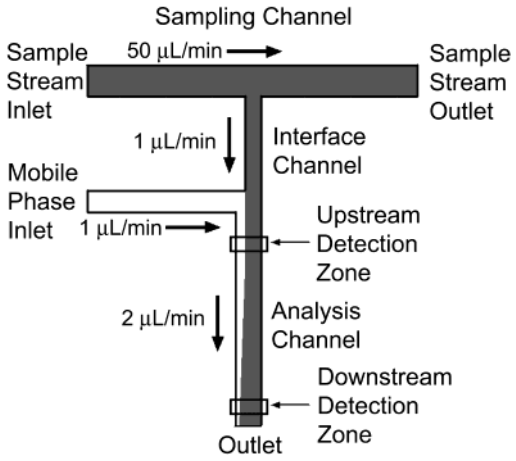

Figure 2. Schematic of the microfluidic network used in these experiments. The sampling channel has sample flow through it introduced by an autoinjector and syringe pump located off-chip to a waste collection also located off-chip. The interface channel is the channel that transports sample from the sampling channel to the analysis channel. Mobile phase is introduced into the analysis channel from a syringe pump and shut-off valve. In the analysis channel, mobile phase and sample merge and pass through an upstream detection region located 500 μm past the merging point of the two streams. The merging mobile-phase and sample streams travel further down the analysis channel to a downstream detection region located 3 cm past the initial merging point of the two streams and out to an off-chip waste collection.

It is instructive to relate the sensor function in the context of the shape of the sample profile entering the sensor. As an analyte concentration profile (peak, plug, steady-state, slowly changing, etc.) enters the sampling channel defined by a sampling channel time scale (Figures 2 and 3), the concentration of the analyte at any instant in time passing through the sampling channel is *compared* by the μ-MWS at two detection zones. Now, in the context of FIA principles, the operative time scale in the analysis channel (e.g., 3 s) is much shorter than the operative time scale in the system providing sample to the sampling channel (e.g., minute(s) to hour(s)). Therefore, for a given analyte concentration entering the analysis channel at any instant in sampling channel time, the μ-MWS provides essentially a steady-state measure of analyte diffusion at the two detection positions. Thus, the short operative time scale in the analysis channel provides an advantage over common FIA methods to measure diffusion. In practice, the data collected at the two detection zones are readjusted to offset the delay time between the two detection zones (e.g., 3 s), so the same sample slice entering the analysis channel is properly compared in calculating the signal ratio as described in the previous paragraph.

EXPERIMENTAL SECTION

System Construction. The experimental design of the RIG detection employed in the μ-MWS is shown in Figure 3 and is similar to the previously reported design[33] with the exception that there are two detection zones applied in this device instead of

(34) Gaffney, C.; Chau, C. K. *Am. J. Phys.* **2001**, *69*, 821−825.

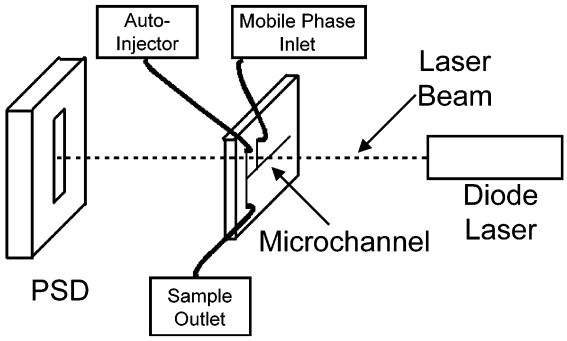

Figure 3. Illustration of the experimental setup. A laser diode beam is focused onto the microchannel and continues through the microfluidic chip onto a position-sensitive detector (PSD) where the deflection of the beam is measured. The laser diode, microchannel and PSD are secured on an optical benchtop and enclosed in a housing built in-house. The microchannel and PSD are also mounted on 3D translational stages to facilitate the alignment of the laser beam to the microchannel and to the PSD. Two syringe pumps are used to deliver the mobile-phase flow and the sampling flow. An off-chip autoinjector introduces sample plugs via the sampling flow onto the microfluidic chip, while a computer controls sample injections and collects data from the PSD.

one. A 5-mW, 780-nm single-mode diode laser (Spindler & Hoyer, DL25, Gottingen, Germany) is focused to a beam diameter of ~160 μm with an objective lens (Spindler & Hoyer, DL25; focal length 16.85 cm). The laser beam was focused onto a poly(dimethyl siloxane) (PDMS) microchannel (made in-house), which was mounted on a high-precision $x-y-z$ translational stage (Newport Corp., 460-x-y-z, Fountain Valley, CA) to facilitate channel alignment, at a distance of 18 cm from the diode laser. The 18-cm distance was previously found to be optimized for this optical configuration.[33] The diode laser beam passed through the PDMS microchannel and was detected on a one-dimensional position-sensitive detector (PSD) (Hamamatsu, S1352, Hamamatsu, Japan). The PSD dimensions were 33 mm × 2 mm where the long side of the PSD was mounted on a high-precision $x-y-z$ translational stage, orthogonal to the microchannel, also at a distance of 18 cm from the microchannel. The deflection of the diode laser beam was then monitored by the long axis of the PSD and read into a PC by a data acquisition board (DAQ; National Instruments, SCB-68, Austin, TX). Analyte was injected onto the microchip by an eight-port autoinjection value (Rheodyne, LabPRO, Rohnert Park, CA), which was controlled through the DAQ board. Data acquisition and instrument control software was written in-house with LabVIEW software (National Instruments, LabVIEW student version 6i). The diode laser, microchannel structure, and PSD were mounted on a standard 5 ft × 2 ft optical breadboard (Newport Corp.) with a foam base and enclosed in a housing (made in-house) to minimize noise due to vibration, stray light, and temperature fluctuations.

Microchannel Design, Fluid Control, and Detection Optimization. The channel design in Figure 2 has channels of varying cross-sectional area allowing the flow rates in the channels to be different. The analysis channel dimensions were 100 μm × 30 μm × 3.3 cm, the sampling channel dimensions were 300 μm × 30 μm × 4 cm, the mobile-phase inlet dimensions were 100 μm × 30 μm × 2 cm, and the interface channel dimensions were 30 μm × 30 μm × 1 cm. The flow rates were controlled to provide a situation where the mobile phase and a portion of the sample stream simultaneously flow down the analysis channel. The μ-MWS had a flow rate of 50 μL/min entering the sampling channel and 49 μL/min exiting the sampling channel, 1 μL/min each through the mobile-phase inlet and interface channels, and thus 2 μL/min through the analysis channel. This allows the two flows to be balanced between sample and mobile phase adjacent to each other down the analysis channel. A total volumetric flow rate through the analysis channel was found to be 2 μL/min by carefully measuring the waste collected from the analysis channel over a period of several hours and correcting for evaporation, giving a linear flow velocity through the analysis channel of 1.1 cm/s.

The microchannels used in this experiment were made in-house using soft lithography techniques that have been previously reported [35−37] and will only be briefly described in this paper. The channels were made in PDMS (Sylgard 184, Dow Corning, Midland, MI) by bonding a patterned piece of PDMS to a blank piece of PDMS and then mounting this construct onto a glass slide. The PDMS surface groups on both pieces of polymer were activated by plasma (Branson International Plasma Corp., Hayward, CA) to facilitate formation of the PDMS bonds. Fluids were transported into the microchannels using two syringe pumps (Isco Inc., μLC-500, Lincoln, NE) via PEEK tubing (Upchurch Scientific, Oak Harbor, WA). Interconnects were made where one end of the PEEK tubing was sealed to the microchannel with epoxy (Epoxy Technology Inc, H74F, Billerica, MA) and the other was connected to the syringe pump with superflangless HPLC fittings (Upchurch Scientific). A PEEK shutoff valve (Upchurch Scientific) was installed between the mobile-phase pump and the microchannel to allow the mobile-phase flow to be easily stopped, if desired, during an experiment.

The sensor was configured as shown in Figures 1−3 so the diode laser beam would be incident upon the analysis channel orthogonal to both the direction of flow and the concentration gradient. The mobile-phase inlet and analysis channel are both in the same plane relative to the incident laser beam. The laser was first visually aligned with the channel, and then the optimum probing position of the channel was determined. The optimum working position was determined by using a dilute sucrose solution where a series of injections were made while the channel position was moved 10 μm between each injection. The optimum position was that position providing a maximum signal-to-noise ratio.[33] This optimization process was repeated each time the channel was moved or any time a new channel was used. Confirmation that the detected signal was due to a RIG detection mechanism was also performed, with results consistent with our previous report.[33] All data were analyzed using ORIGIN software (Microcal Software, Northampton, MA).

Polymer Experiments. PEG solutions were made at a concentration of 5 ppth (parts-per-thousand, w/v) using PEG standards (Polymer Laboratories, Amherst, MA) from a molecular weight of 106 to 22 000 (see Table 1). Experiments were repeated

(35) Xia, Y.; Whitesides, G. M. *Angew. Chem., Int. Ed. Engl.* **1998**, *38*, 550−575.
(36) Duffy, D. C.; McDonald, J. C.; Schueler, O. J. A.; Whitesides, G. M. *Anal. Chem.* **998**, *70*, 4974−4984.
(37) Vahey, P. G.; Park, S. H.; Marquardt, B. J.; Xia, Y.; Burgess, L. W.; Synovec, R. E. *Talanta* **2000**, *51*, 1205−1212.

Table 1. PEG Standards Used in These Experiments with Their Molecular Weight and Diffusion Coefficient Calculated from Eq 4

poly(ethylene glycol) samples	molecular weight	diffusion coefficient D_m ($\times 10^{-7}$ cm^2/s)
PEG 106	106	96.2
PEG 194	194	69.0
PEG 440	440	44.0
PEG 600	600	37.1
PEG 960	960	28.6
PEG 1470	1470	22.6
PEG 4120	4120	12.8
PEG 7130	7130	9.50
PEG 8500	8500	8.62
PEG 11840	11840	7.19
PEG 22800	22800	5.01

3 times for each different PEG solution at both the upstream and downstream detection positions, over a period of 2 days. The upstream position was located ~500 μm past the initial merging point of the sample and mobile-phase flows, and all the data at this position were collected on 1 day. The channel mount was then repositioned in relation to the laser beam to the downstream position, which was located 3 cm downstream from the initial merging point, giving a ~3-cm distance between the two detection regions. All the data collected at the downstream position were collected using the same solutions as the previous day. Both the upstream and downstream data were collected after optimizing the incident diode laser beam position to provide optimum sensitivity. Thus, great care was taken to ensure that the two data sets could be objectively compared. For the work reported here, collection of the two data sets in this fashion was reasonable for the proof of concept for the μ-MWS idea. Ideally, and in the future, the device will be designed so the upstream and downstream measurements are obtained simultaneously with a dual-beam/dual-PSD design.

RESULTS AND DISCUSSION

We now turn our attention to the development of this RIG detector as an integral component of the μ-MWS. The μ-MWS functions by correlating the diffusion behavior of a class of compounds of interest to their molecular weight. By obtaining RIG measurements at two different positions along the analysis channel as in Figure 2, the required data to make the correlation is provided. The first detection position (upstream) is just past the merging point of the two flow streams, i.e., past the entrance of the mobile-phase and sample interface channels. The second detection position (downstream) is much further down the channel, closer to the outlet, where the sample has had time to diffuse into the mobile phase. Table 1 lists the PEG standards that were used in these experiments with their molecular weight and diffusion coefficient, D_m (in cm^2/s), related according to eq 4,[32] where MW is the average molecular weight of a PEG assumed

$$D_{m,PEG} = 1.25 \times 10^{-4}(MW)^{-0.55} \quad (4)$$

to behave as a random coil. The impact of molecular diffusion is to provide two different signals at the two detection regions, for the same analyte solution, from which a correlation can be made

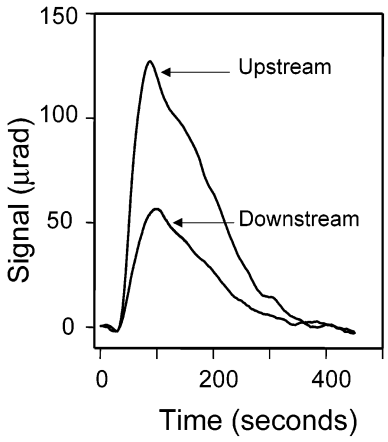

Figure 4. Signal versus time plot for 100-μL off-chip injection of PEG standard of 11 840 molecular weight at an injected concentration of 5 ppth (w/v). The peak shape can be attributed to the FIA hydrodynamic conditions under which the sample is delivered to the sensor chip. (a) PEG monitored at the upstream detection region (Figure 2). (b) An injection of the same solution monitored at the downstream detection region (Figure 2), 3 cm downstream from upstream detection position. The data collected for the upstream peak have been aligned along the time axis, initially with a lag time of 3 s, with the data for the downstream peak so both peaks have the same starting time.

between diffusion and molecular weight. In practice, one would need to establish eq 4 for each compound class of interest, analogous to the practice of size exclusion chromatography. The correlation between D_m and MW is made through the hydrodynamic radius of the molecules of interest. For example, one would expect a marked difference in the numerical coefficients in eq 4 for random coils versus asymmetrically shaped molecules (e.g., DNA), yet achieving a useful calibration should not be problematic in either case. We shall see that the correlation between the signal measured at two positions and molecular weight for the PEG samples is reasonably independent of concentration.

To demonstrate the capability of making a correlation to molecular weight, data were collected by making three injections of each of the PEGs listed in Table 1 at a concentration of 5 ppth at the upstream detection position and again at the downstream detection position. Figure 4 shows two peaks collected for the PEG 11840 sample, one at the upstream position and one at the downstream position. Since there is a time delay between the two detection regions, the two peaks have been aligned along the time axis. As expected, the peak collected at the upstream position is larger, with a larger peak height but with a common peak shape. The upstream peak was measured with the incident beam ~500 μm from the initial merging of the mobile-phase and sample interface streams. The larger RIG signal obtained at the upstream position is achieved since the two streams have only recently merged and there is not a significant amount of diffusion of PEG from the sample stream into the mobile-phase stream. Since the downstream detection position was ~3 cm from the upstream position, and the linear flow velocity was 1.1 cm/s, the time for diffusion was ~3 s so the concentration gradient is smaller, resulting in a smaller signal at the downstream position. Note that the 100-μL injection volume for the FIA system delivering a given sample to the μ-MWS was selected so the maximum peak

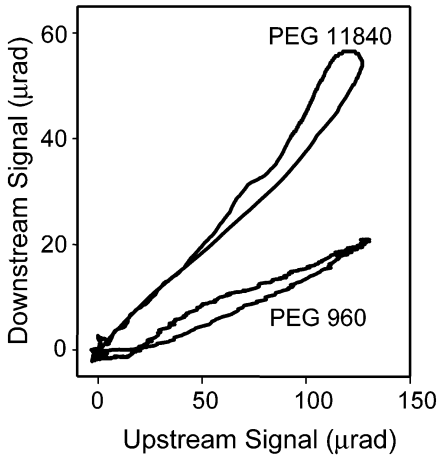

Figure 5. Signal collected at the downstream position versus signal collected at the upstream position for two different molecular weight PEGs to show both molecular size selectivity and concentration independence. Signals are aligned in time to have the same starting point, as shown in Figure 4. All solutions were at an off-chip injected concentration of 5 ppth (w/v) with a 100-μL injection loop. Data collected for 11 840 MW PEG and for 960 MW PEG.

concentration was equal to the injected "steady-state"concentration, yet the analysis time was minimized. This equality was confirmed by injecting a suitably larger sample volume (200 μL) so the signal achieved a steady-state response and then confirming that the peak heights in Figure 4 (using a 100-μL injection) were identical to the steady-state response. Since the 100-μL injection took less time, subsequent samples were run with a 100-μL injection and it is understood that the peak maximum corresponds to the steady-state response.

The limit of detection (LOD) was calculated from data collected for three replicate baseline runs and three replicate runs of PEG 11840 at both the upstream and downstream positions. The LOD was taken to be 3σ of the baseline noise for 400-s sections of baseline. The calculation was performed on three different data sets to obtain an average LOD of 56 ppm with a standard deviation of $\pm$1.9 for the upstream position and 119 ppm with a standard deviation of $\pm$1.4 for the downstream position. The index of refraction of a 1% aqueous PEG 11840 solution was measured and the dn/dC of the PEG was determined to be 8×10^{-8} RI ppm^{-1}. The LOD in terms of the angle of deflection was determined to be 1.43 $\pm$ 0.34 μrad. Thus, the LOD in terms of ΔRI was determined to be 4.5×10^{-6} RI at the upstream position and 9.5×10^{-6} RI at the downstream position. Note that the RI LOD is effectively a function of the analyte diffusion coefficient and time allowed for transverse diffusion to occur within the analysis channel.

Another useful approach to plot the data, initially in the form presented in Figure 4, is to make a plot of the downstream signal versus the upstream signal of the aligned peaks for a given PEG. Two different molecular weight PEGs have been plotted in this fashion in Figure 5. Indeed, the data for PEG 11840 shown in Figure 5 are the same as that used in Figure 4. Displaying the data in this manner is similar to producing a calibration curve for each different polymer, and the slope of each plot is a function of the PEG diffusion coefficient. The injection volume for the FIA system delivering the PEG samples to the μ-MWS was designed so the maximum peak concentration was equal to the injected concentration (5 ppth). Thus, for each PEG signal, the detected peak begins at a concentration of 0 ppth, reaching 5 ppth at the peak, and then decreasing back to the baseline of 0 ppth. Thus, each point along the plot for a given PEG in Figure 5 corresponds to a concentration within the range of 0−5 ppth. An important feature of a molecular weight analyzer such as the μ-MWS is that the diffusion behavior of the analyte should ideally be independent of concentration. This can be seen in Figure 5, where the downstream signal versus the upstream signal plot for two samples, PEG 11840 and PEG 960, both track up and down along a unique, approximately linear function within the limits of experimental error. If the diffusion coefficient dependence of the RIG signal for a given PEG was completely independent of concentration, then the data in Figure 5 should track out along a perfectly straight line reaching a maximum and then track back to zero along the same line. On the other hand, since the magnitude of the RIG signal is related to the concentration gradient, which is in turn dependent on the analyte diffusion coefficient, a line with a different slope would be obtained for analytes with different diffusion coefficients. The plots for each PEG in Figure 5 are sufficiently unique and linear that both PEGs with different molecular weights can easily be identified. Future work with a dual-beam/dual-PSD design will provide additional evidence to interrogate the linearity and uniqueness issue further. All PEGs in Table 1 provided similar behavior when plotted like the two PEGs in Figure 5 but are not shown for clarity. Instead, to study the trend for all PEGs, the upstream and downstream peak areas for each sample were determined from data as shown in Figure 4 and studied further. These results will now be presented.

The average peak area versus molecular weight plot is shown in Figure 6a for all the PEGs in Table 1, injected at 5 ppth, at both the upstream and downstream positions. For a peak area measurement, a baseline is defined and set to 0 (i.e., from 0 to 400 s in Figure 4), and the peak is integrated using Origin software. Figure 6a demonstrates peak area is affected by molecular weight (i.e., diffusion) at the two different detection positions. This idea can be generalized such that one could measure the RIG at a variety of positions along the merging flows in the analysis channel in order to broaden the molecular weight range analyzed. At the upstream detection position, the faster diffusing, lower molecular weight, polymers show a significant trend in molecular weight selectivity, shown in Figure 6b, while the slower diffusing, larger molecular weight, polymers essentially plateau with a higher RIG signal. Since all of the PEGs have essentially the same RI, and each solution is at the same concentration and injected volume, the difference in sensitivity can be completely attributed to the difference in diffusion. Thus, the ability of the μ-MWS to distinguish molecules with different diffusion coefficients is further demonstrated. The fast diffusing, smaller PEGs produce a smaller signal as the concentration gradient is reduced relative to the slower diffusing larger PEGs. The data collected at the downstream detection position show that the faster diffusing, smaller polymers have almost completely equilibrated across the microscale analysis channel so there is very little RIG signal present. As with the upstream data, the concentration gradient, and thus the RIG signal, increase as the molecular weight increases. However, the downstream data do

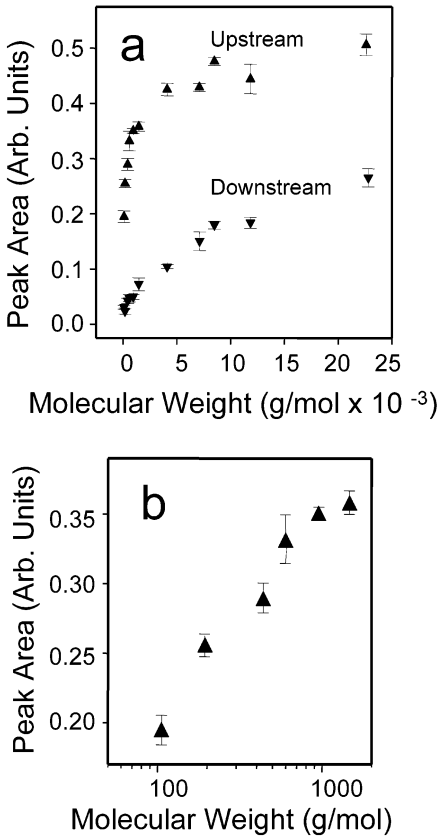

Figure 6. Average peak area as a function of molecular weight for PEG standards at an injected concentration of 5 ppth. (a) Average for three runs collected for 100-μL injections of PEG solutions at the upstream position, and average for three runs collected for 100-μL injections of PEG solutions at the downstream position. Error bars are $\pm$ one standard deviation. (b) Expanded view of the average peak area as a function of molecular weight (log scale) for the smaller PEG standards collected at the upstream detection position. Excellent molecular weight selectivity for the smaller molecules is demonstrated. Error bars are $\pm$ one standard deviation.

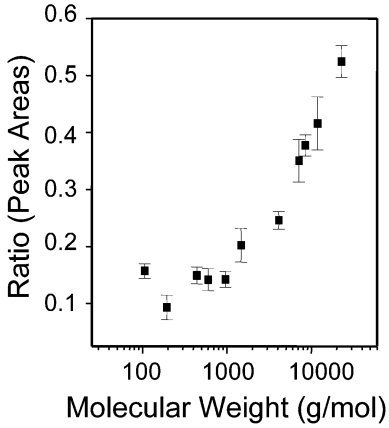

Figure 7. Ratio of the peak areas (downstream signal area/upstream signal area) as a function of molecular weight (log scale) of the PEG at an injected concentration of 5 ppth (w/v). Ratio is calculated for three runs at each position and the average is then taken for each molecular weight, with the error bars $\pm$ one standard deviation.

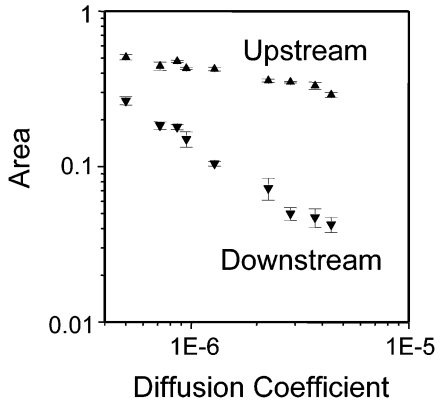

Figure 8. Peak area (log scale) versus diffusion coefficient (log scale) for PEGs at the upstream and downstream detection positions. Points represent the average values of data collected over three runs of each molecular weight PEG solution at an injected concentration of 5 ppth (w/v). The error bars are $\pm$ one standard deviation.

not show the same leveling off behavior with the larger polymers as seen at the upstream position. Thus, there is considerably more molecular weight selectivity for the larger PEGs at the downstream detection position. It is likely that, at the upstream position, the larger PEGs are providing a maximum RIG sensitivity in which the concentration gradient is essentially near optimum in the context of the limitations of the optical configuration.

The data in Figure 6 are still a function of concentration. A more useful way to view the data is to take the ratio of the downstream peak area divided by the upstream peak area and plot this ratio versus molecular weight shown in Figure 7. Here, it can be seen that the lower molecular weight polymers are more difficult to distinguish from one another while the samples ranging from 960 to 22 800 are readily distinguishable. By taking the ratio of the downstream-to-upstream signals, information is provided that is independent of the injected sample concentration. Again, in principle, the device can be designed to make the upstream and downstream measurements simultaneously, and the molecular weight range should be readily tuned either by adjusting the distance separating the two detection positions or by adjusting the linear flow velocity in the detection region. Since optical alignment is needed to adjust the distance separating the detection zones, and it is a somewhat time-consuming process at this stage, then tuning flow rate is likely to be easier to implement. Note that flow rate changes, if unplanned, will be a source of uncertainty in the molecular weight determination. Flow rate monitoring and control, as well as improved design of the channel structure flow paths, is warranted to minimize the potential adverse effect of flow rate variation. In a process monitoring application, for example, the analyst would need to develop a calibration protocol, involving running standards in a matrix similar to the sample of interest and implement flow rate monitoring to ensure the time between measurements at the two detection positions is kept under control. While the data presented support a proof of concept, it is also the impetus for future work.

The data collected by the μ-MWS can also be evaluated by relating the peak area as a function of the diffusion coefficient of the analyte of interest. Figure 8 shows a plot of the peak area versus diffusion coefficient for the upstream data and the downstream data. Examining either the upstream or downstream data alone, as a function of diffusion coefficient, leads one to consider the possibility that a simple, single-exponential rate law for diffusion may be insufficient to explain the observed response of

the device, which corroborates a previous report.[38] Continued investigation of the phenomenon at work and understanding how to tune the device to the optimal detection zone locations should improve the range over which the μ-MWS can make molecular weight determinations.

CONCLUSIONS

The μ-MWS clearly shows an ability to make molecular weight determinations. However, more work is warranted to learn how to optimize performance. The current work demonstrated the principle of dual-position RIG detection, while future work is aimed at taking the next step to design, produce, and examine a device that makes both the upstream and downstream measurements in real time. Thus, the ratio can also be provided in near-real time, defined by the linear flow velocity and distance separating the two detection regions. The next-generation device requires two PDSs both orthogonal to the *z* axis (Figure 1), to obtain two channels of data that can have their ratio taken for the purpose of removing the concentration dependence prior to relating to a molecular weight calibration (Figure 7). Continued development of this sensor will focus on optimizing the molecular weight range through detection zone location selection and flow rate manipulation. The inherently small volume associated with the microfluidic device offers the ability to do continuous real-time sampling of a variety of processes. Furthermore, the μ-MWS shows promise as a detector for liquid chromatography (LC) methods, such as size exclusion chromatography, reversed-phase LC, and ion-exchange chromatography. In applications with LC, the μ-MWS should prove complementary to light-scattering detection[5−7] since the μ-MWS appears better suited to low molecular weight analytes.

(38) Kamholz, A. E.; Yager, P. *Sens. Actuators, B* **2002**, *82*, 117−121.

ACKNOWLEDGMENT

We thank the Center for Process Analytical Chemistry (CPAC), a National Science Foundation initiated University/Industry Cooperative Research Center at the University of Washington, for financial support. We also thank Wes Quigley of the University of Washington for insightful discussions and advice.

Received for review March 5, 2002. Accepted June 20, 2002.

AC020143Z